Studying batteries with Electrochemical Impedance Spectroscopy (EIS)

I – INTRODUCTION

Measuring the impedance of batteries is not a new idea. Early measurements were performed in 1963 on a Leclanché battery [1]. A review on this subject from 1998 is listing 61 papers [2]. Patents from 1973 can also be found by the dozens on the subject of charge control [3]. Some examples are given in the reference list [4-7]. Nowadays, performing a literature review on this subject seems impossible due to the abundance of the publications.

Impedance measurements are used to study each part of the battery: the electrodes, the separator or electrolyte. However, the most frequent use of impedance is to determine the State of Charge (SoC) of the battery as well as the degradation of its performance with cycling. Such studies are of interest for BMS (Battery Management System) development as well as quality testing. Impedance studies are recommended by the US Department of Energy for the development and testing of batteries for EVs (Electrical Vehicles) [8].

The aim of this paper is to explain, as simply as possible, why EIS is interesting for battery testing and battery studies.

Firstly, we will compare the advantage of dynamic studies *vs.* static studies and secondly, introduce the specific case of batteries and how impedance data can be used.

II – STATIC REGIME AND DYNAMIC REGIME

I - 1 ELECTRICAL CIRCUIT

Let us consider the electrical circuit of test circuit #3.1 (Fig. 1). More information is given in [9-10]. The corresponding steady-state curve and the Nyquist diagram of the impedance measured at points a and b of the steady-state curve are shown in Fig. 2.

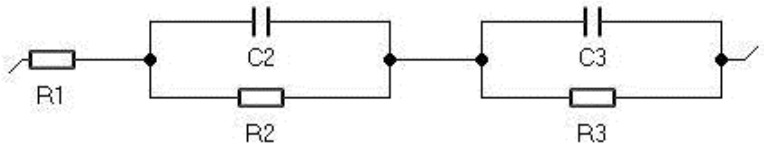


Fig. 1: Circuit R1+C2/R2+C3/R3.

Measuring the DC current only gives access to the sum of the resistances *R*1, *R*2 and *R*3 using Ohm's law

$$U = (R1 + R2 + R3)/I \qquad (1)$$

With *U* the applied potential and *I* the current through the circuit.

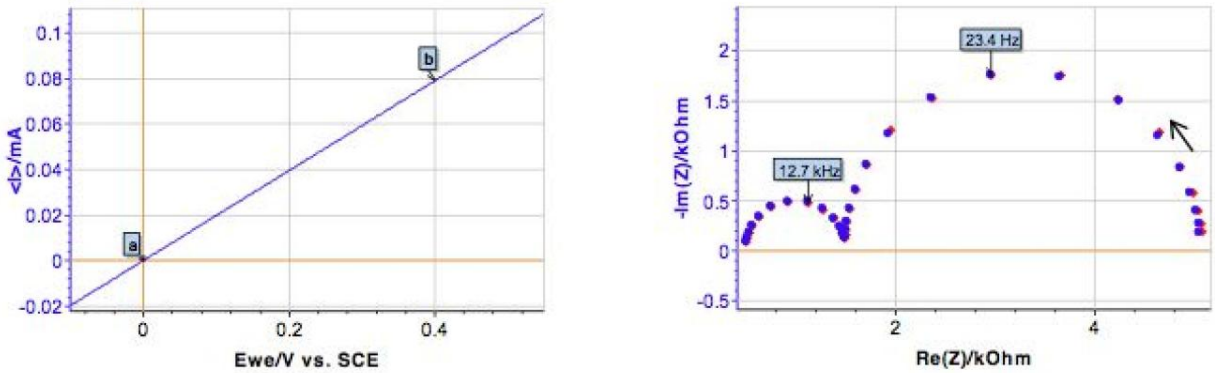


Fig. 2: Steady-state curve and Nyquist diagram for the impedance. Impedance is measured at steady-state points a and b. The arrow indicates increasing frequencies.

An impedance measurement at a suitable frequency range around U = 0 V can lead to the measurement of $R1$, $R2$ and $R3$, as well as the determination of the values of the capacitors $C2$ and $C3$. This can be done directly without any fitting operation.
As such, this result is enough to justify the use of EIS for batteries, supercapacitors, fuel cells, electrolyzers and other electrochemical systems. EIS can give a more complete description of a system.

I - 2 THE CASE OF THE BATTERY

During a discharge or a charge of a battery at a constant current what can only be measured is the potential difference $U(t)$[1] as a function of time (Fig. 3). The only way to analyze these data is to use Ohm's law and to determine what is sometimes named "direct current resistance" [11-12].

$$R_{DCR}(t) = U(t)/I \qquad (2)$$

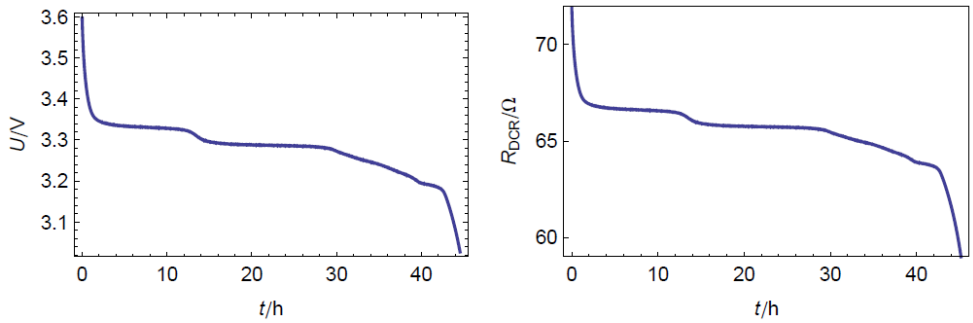


Figure 3: Example of a discharge curve of a Li-ion battery ($I_{discharge}$ = 50 mA) (left) and evolution of the direct-current resistance (right).

Impedance measurements can be performed on a battery at Open Circuit Voltage (OCV) or under operation (charge or discharge), most preferably in current control mode, *i.e.* galvanostatic mode [13]. An example of impedance graph measured on a Li-ion battery is shown in Fig. 4. This graph is composed of a linear part at lower frequencies (LF) with an arc at intermediate frequencies (MF) and an inductive part at higher frequencies (HF). More details about how to interpret these graphs are given in Bio-Logic application notes #61 and #62 [27,28].

[1] Noted Ecell in EC-Lab®

Many examples of experimental graphs can be found in Bio-Logic application and technical notes [13-17]. The impedance graph shown in Fig. 4 contains more information than the electromotive force (emf, ie the voltage difference at OCV) of a battery or the evolution of R_{DCR}.

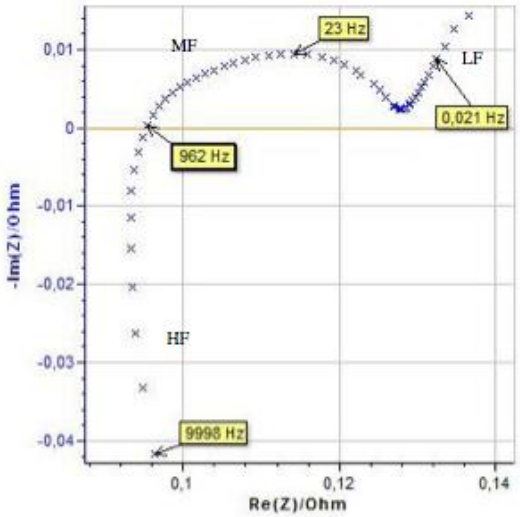


Figure 4: Example of an impedance graph of a Li-ion battery. Measurement performed at OCV: emf = 3.844 V.

III – IMPEDANCE OF BATTERIES

III - 1 ANALYSIS OF IMPEDANCE GRAPHS

Measuring an impedance graph of a battery is quite easy using an EIS modelling tool (for example Z Fit, available EC-Lab®, BT-Lab® or MT-Lab®), but analyzing experimental results can happen to be more difficult. The circuit of the TestBox #3.1 is known by construction but analyzing the impedance graph of an electrochemical system requires the use of electrical equivalent circuits, that one needs to choose.

These electrical equivalent circuits are either induced from the identification of characteristic shapes of the impedance graphs of basic electrical elements such as R/C or R/Q circuits, diffusion impedance and so on... or deduced from the modelling of electrochemical reactions occurring at the electrodes. The first type of modelling is electrical and the second is electrochemical. Sometimes modelling is mixed and involves both electrical and electrochemical components.

III - 2 MODELLING IN TERMS OF EQUIVALENT CIRCUITS (ECs)

a. Impedance graphs fitting

Many Equivalent Circuits (EC) are offered in the literature to analyse batteries impedance graphs. Four of them are shown in Fig. 5.

Circuits (1), (2) and (4) neglect the inductive part at higher frequencies[2].

Adding a circuit L/R and replacing W4 by Q4 in circuit (2), we have the following circuit: R1+L2/R2+Q3/R3+Q4/R4+Q5 (Fig. 6) that can be used *a priori* to fit impedance graphs shown in Fig. 4 or in Fig. 7.

It is not necessary to suggest or attribute a physical meaning of the components of this circuit to be able to use it to fit the impedance graph. It is a major advantage and a major limitation of using ECs. For example, the Q5 component at lower frequencies does not have any physical meaning but

[2] The HF inductive part is sometimes concealed by the fact that only the top right part of the complex plane is shown.

allows to correctly fit the data. Once an equivalent circuit is chosen, fitting is very easy using Z Fit available in EC-Lab ® or BT-Lab ®. More information on the fitting of low frequency data are given in [27].
A rough scheme interpretation of the different parts of a typical impedance graph is given in Fig. 8.

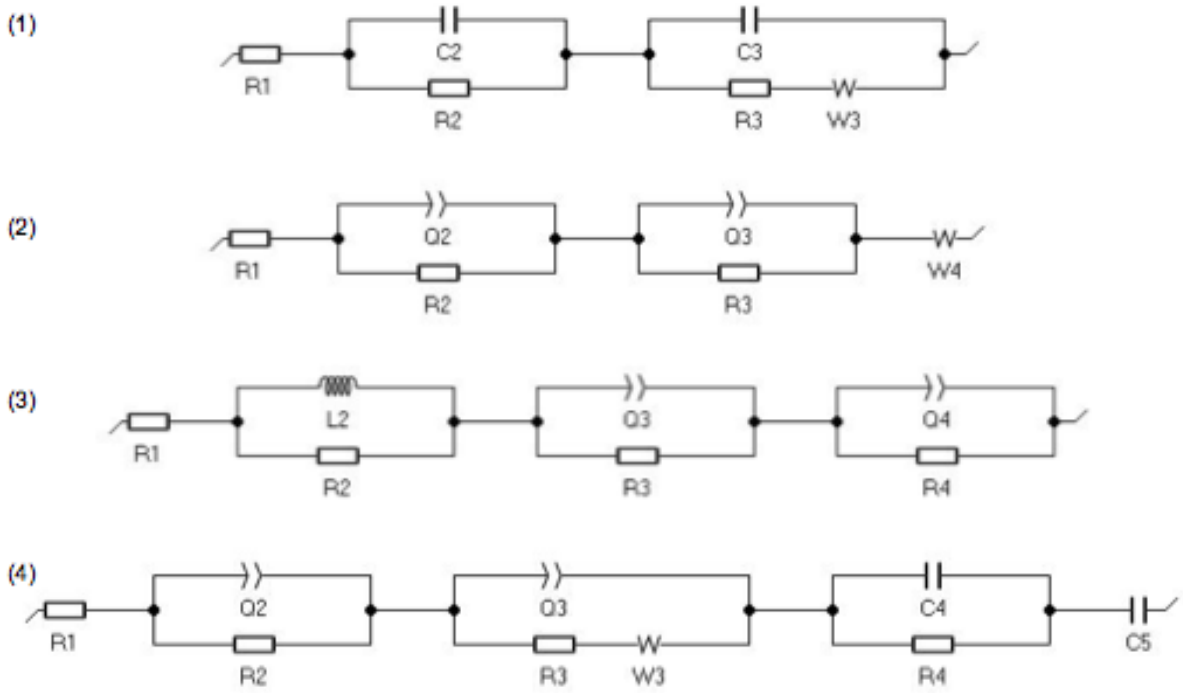


Figure 5: Some ECs used for fitting impedance data of batteries. From top to bottom [18-21].

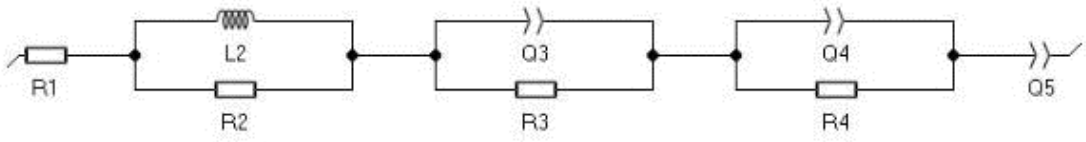


Figure 6: Equivalent circuit R1+L2/R2+Q3/R3+Q4/R4+Q5.

b. Variation of the values of the parameters with the State of Charge (SoC) or State of Health (SoH)

Impedance graphs measured on a Li-ion battery are shown in Fig. 7, for an almost completely charged (SoC ≈ 80%) and discharged (SoC ≈ 10%) battery. The general shape of the graph is the same. The arc at intermediate frequencies corresponds to the coalescence of two arcs when the battery is almost entirely discharged. Whatever the frequency, the modulus of the impedance increases with the depth of discharge (Fig. 9)[3].
Figure 10 shows the results obtained by fitting the impedance graphs of Fig. 7 with the electrical circuit shown in Fig. 6. The values of the resistances R1, R2 and R3 are presented in Tab. I.

[3] It must be noted that the impedance is a complex number and there is no natural linear ordering in the set of complex numbers. Hence, saying "This impedance increases" or "This impedance is larger than that one" is erroneous. Comparing moduli is correct because the moduli belong to the set of real numbers.

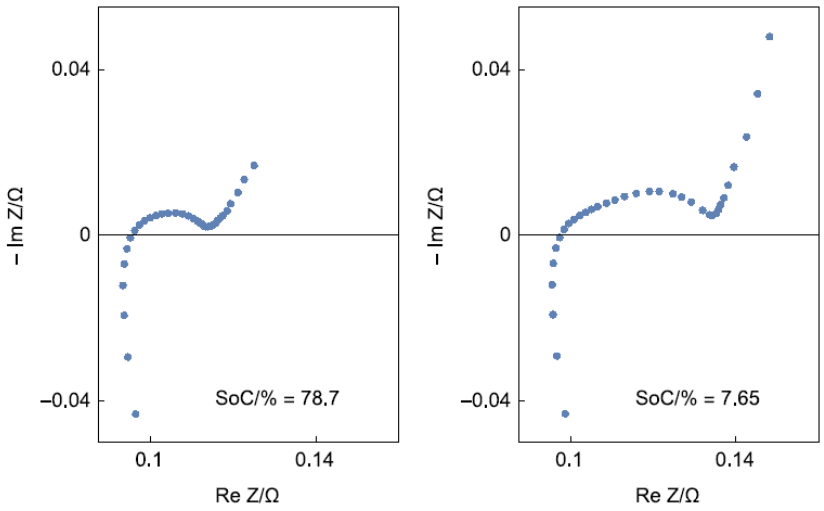


Figure 7: Impedance graphs of a battery at two different SoC measured under the same conditions.

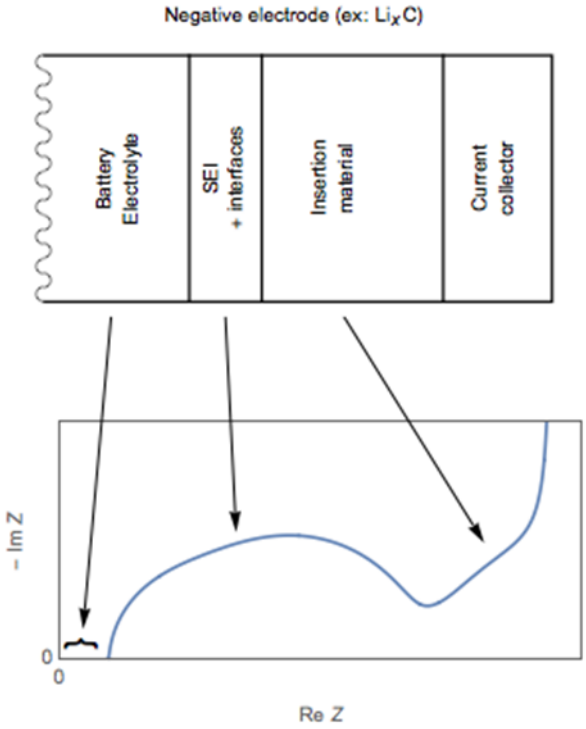


Figure 8: Rough scheme of a half-battery, showing how to interpret the different parts of an impedance graph.

Table I: Change of *R*1, *R*2 and *R*3 values with SoC.

SOC	R1/Ω	R2/Ω	R3/Ω
80%	9.12×10^{-2}	6.61×10^{-3}	2.28×10^{-2}
20%	9.37×10^{-2}	1.44×10^{-2}	2.70×10^{-2}

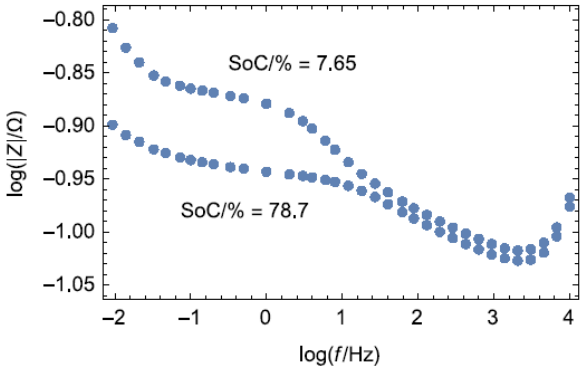


Figure 9: Impedance moduli of Fig. 7.

For a given frequency, the values of the impedance modulus change with SoC. It is therefore possible to monitor the evolution of the values of the components of an EC with the SoC of a battery and search for empirical variation laws of the values of the components:

$$R_i = f(\text{SoC}) \qquad (3)$$

where R_i is either the modulus of the impedance or the real part of the impedance at a given frequency. Using the R_i vs. SoC curve one can deduce SoC by measuring R_i.
It must be noted that the function f in Eq. (3) is dependent on the chemistry of the battery (or battery technology).

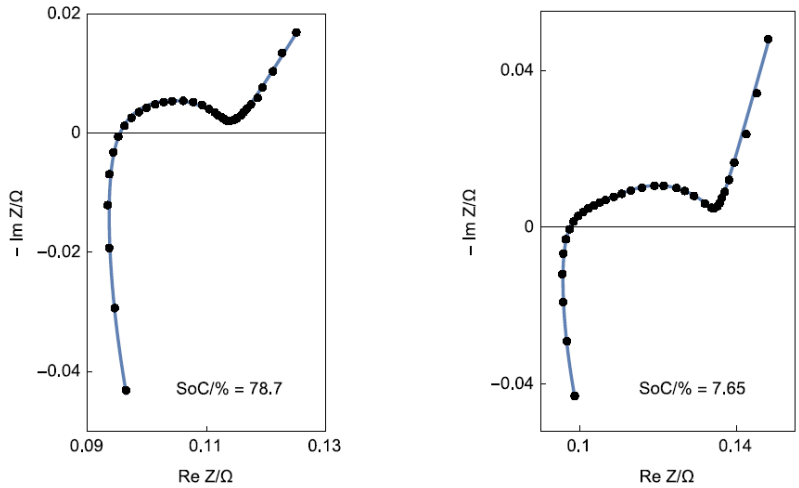


Figure 10: Fitting of the impedance graphs from Fig. 7 using EC shown in Fig. 6.

Cycling the battery allows to study the evolution of the values of the components with the cycle numbers and consequently the State of Health (SoH). It is then possible to search variation laws such as:

$$R_i = f(\text{SoC, SoH}) \qquad (4)$$

Empirical laws can be used to test SoC and SoH. This empirical approach can be performed without giving physical meaning to the components of ECs and does not offer physical ground for these correlations. Only the electrochemical modelling of the reactions occurring at the two electrodes of a battery allow one to give physical justifications for behavior laws of batteries.

III - 3 MODELLING IN TERMS OF AN ELECTROCHEMICAL REACTION

a. *Introduction*

A battery is the series association of a positive electrode, a separator and a negative electrode[4]. The impedance of a battery writes:

$$Z = Z_+ + Z_- + R_{sep} \qquad (5)$$

Where Z_+, Z_- R_{sep} are the impedance of the positive electrode, the impedance of the negative electrode and the resistance of the separator, respectively.
Some batteries, for example Li-ion batteries can exhibit an additional component, for example the Solid Electrolyte Interphase, which is formed during the first charge by reduction of the organic electrolyte. This SEI is usually modelled by an R/C component.

b. *Impedance of positive and negative electrodes*

The electrochemical reactions that take place at the electrode of a battery depend on the battery type, that is to say, on the electrode materials and electrolytes. The reactions taking place at the electrode of a lead battery do not have the same physico-chemical nature as the ones taking place at the electrodes of an Li-ion battery. Modern batteries often involve insertion reactions, as it is the case for Li-ion batteries. Insertion reactions can also have several steps [22].

c. *Direct insertion*

The direct insertion reaction, represented in Fig. 11, along with its equivalent circuit writes:

$$M^+ + \langle\ \rangle + e^- \underset{K_o}{\overset{K_r}{\leftrightarrow}} \langle M \rangle \qquad (6)$$

The faradaic impedance $Z_f(f)$ writes [5]

$$Z_f(f) = R_t + R_{\langle M \rangle} \frac{\coth \sqrt{\tau_{d\langle M \rangle} i2\pi f}}{\sqrt{\tau_{d\langle M \rangle} i2\pi f}} \qquad (7)$$

Detailed relationships are given in [22]. Figure 11 shows a typical impedance graph of a direct insertion reaction. It is composed, from low to high frequencies, of a capacitive part, followed by a linear part forming an angle of -π/4 with the real axis and finally a semi-circle, or an arc when the double-layer capacitor is replaced by a Constant Phase Element (CPE). The variation of R_t and R_{in} with potential E is shown in Fig. 12.

Insertion reactions are not always that simple. They can be composed of several processes [22] and insertion materials can be composed of various phases.

[4] These electrodes are sometimes referred to as anode or cathode. The negative electrode of an accumulator works as an anode during discharge and as a cathode during charge, whereas the positive electrode works as a cathode during discharge and as an anode during charge. At OCV, the electrodes are neither anode or cathode.
[5] The expressions of the impedance of elements Ma and Mg from EC-Lab®could be used instead of the expression of the impedance of the element M.

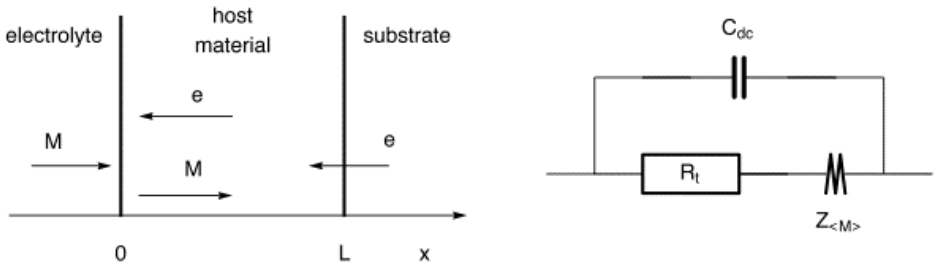


Fig. 11: Scheme of the direct insertion reaction. Hypotheses: planar electrode no transport limitation of M^+ in the electrolyte, linear restricted diffusion of the inserted species ⟨M⟩, isothermal Langmuir insertion: $M^+(0; t) \approx M^{+*}$, $J_{\langle M\rangle}(L, t) = 0$, $K_r = k_r\exp(-\alpha_r fE)$, $K_o = k_o\exp(\alpha_o fE)$ (left). EC of the electrode impedance for the direct insertion reaction with $M^+(0; t) \approx M^{+*}$ and $J_{\langle M\rangle}(L, t) = 0$. The M symbol (restricted diffusion element) designates the element with impedance $Z_{\langle M\rangle}$ (right).

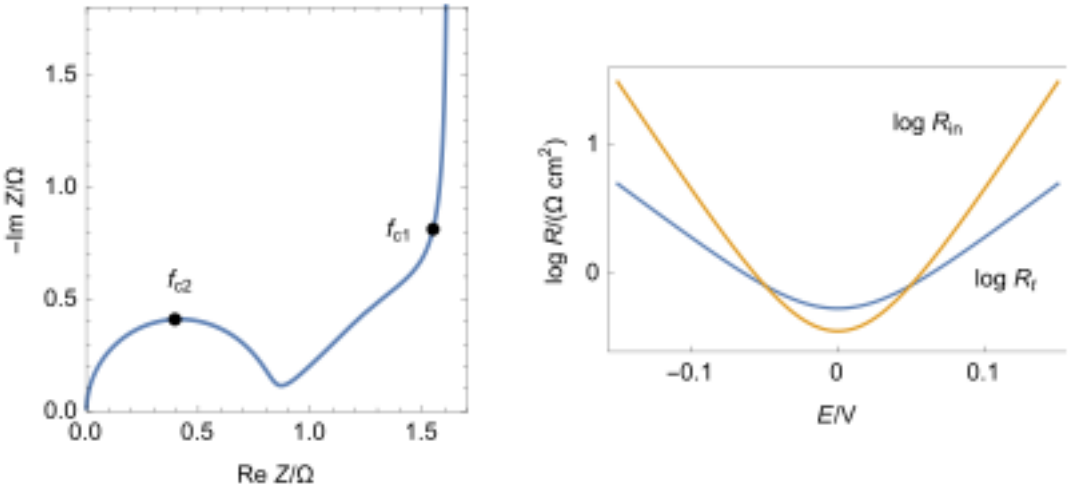


Fig. 12: Typical impedance graph of the direct insertion reaction. $k_o = 10^{-3}$ cm s^{-1} ; $k_r = 1$ mol^{-1} cm^4 s^{-1} (which means $k_o = 10^{-3}$ cm s^{-1} ; $E_o = 0$ V) ; $\alpha_o = \alpha_r = 1/2$; $M^{+*} = 10^{-3}$ mol cm−3 ; $\langle M\rangle_{max} = 10^{-3}$ mol cm^{-3} ; $D_{\langle M\rangle} = 10^{-7}$ cm^2 s^{-1} ; $L = 10^{-4}$ cm ; $C_{dl} = 10^{-5}$ F cm^{-2}. E = 0.05 V. $f_{c1} = 3.88/(2\pi\tau_{d\langle M\rangle})$, $f_{c1} = 3.88/(2\pi R_t C_{dl})$ (left). Evolution of the decimal logs of the transfer resistance and insertion resistance with the electrode voltage for an intermediary electronic transfer (right).

d. Impedance of a battery

The resulting impedance graph of a battery might be quite complicated. The number and the meaning of the impedance arcs depend on the values of the parameters of both electrodes. The impedance graph shown in Fig. 4 was fitted using a circuit comprising two R/Q circuits (Fig. 6). There is no way to attribute one circuit or the other to one or the other electrode. The probability of having different characteristic frequencies of the impedance related to diffusion process is very low.

Impedance graph obtained on a battery with two electrodes setup will be caused by reactions occurring at both electrodes.
This problem could be circumvented by:

- Performing impedance measurements on a battery for which only one electrode is subject to the insertion reaction, for example by choosing a negative electrode made of Li [23] and assuming that the impedance of the former is negligible whatever the frequency.

- Using batteries in which one or several reference electrodes are inserted, which allows the simultaneous of the impedance of both electrodes [1, 25, 26, 29]. An example of an impedance graph measured on a three-electrode battery is shown in Fig. 13.
- Building symmetrical batteries.

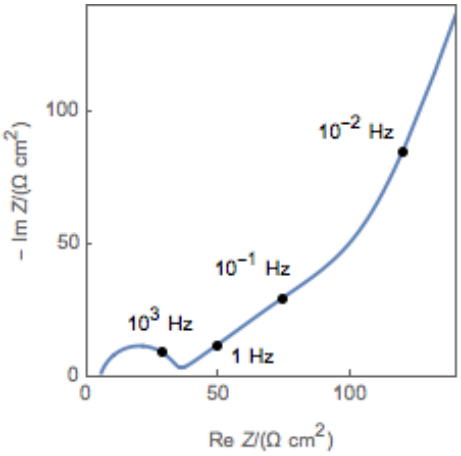


Figure 13: General shape of impedance data taken from [30], calculated using Eq. 6, with the element Ma instead of M.

IV – CONCLUSION

The Electrochemical Impedance Spectroscopy allows us to characterize the dynamic behaviour of electrochemical systems. Two different approaches can be used to analyse the impedance graphs measured on batteries:

- It is is possible to search for correlations between one or several components values from ECs and the SoC/SoH, which can then lead to the implementation of a testing procedure of batteries, which can be furthermore used in the optimization of charge and discharge procedures. This approach is the simpler one but cannot be used as such if an understanding of the phenomena occurring at the electrodes is required.
- It is possible to analyse impedance graph in order to understand electrode reactions, how to optimize them, and understand the phenomena involved in aging. This approach requires the electrochemical modelling of the electrochemical reactions occurring at the electrodes as well as the development of techniques that can help in attributing the impedance arcs to one or the other electrode.

REFERENCES

[1] Ralph J. Brodd and Harold J. DeWane, Impedance of Leclanche cells and batteries, J. Electrochem. Soc. 11 (1963) 1091–1097.

[2] F. Huet, A review of impedance measurements for determination of the state-of-charge or state-of-health of secondary batteries, J. Power Sources 70 (1998) 59–69.

[3] D. Taylor, Impedance controlled battery charger and method of charging with monitoring of a.c. answer signal, US Patent 3,816,807 (Jun. 11 1974).

[4] E. Dowgiallo, Method for determining battery state of charge by measuring a.c. electrical phase angle change, US Patent 3,984,762 (Oct. 5 1976).

[5] R. Mingant, J. Bernard, V. Sauvant-Moynot, In-situ battery diagnosis method using electrochemical impedance spectroscopy, US Patent 8,849,598 (Sep. 30 2014).

[6] A. Christensen, R. Mosbæk, Electrochemical impedance spectroscopy in battery management systems, WO Patent App. PCT/IB2015/055,441 (Jan. 28 2016).

[7] Battery sorting method based on alternating-current impedance spectrum, CN Patent 102,553,838 (May. 7 2014).

[8] https://avt.inl.gov/sites/default/files/pdf/battery/freedomcar_manual_04_15_03.pdf

[9] Application note #14. Zfit and equivalent electrical circuits.

[10] Application note #9. Linear vs. non linear systems in impedance measurements.

[11] C. Fleischer, W. Waag, H.-M. Heyn, D. U. Sauer, On-line adaptive battery impedance parameter and state estimation considering physical principles in reduced order equivalent circuit battery models: Part 1. Requirements, critical review of methods and modeling, J. Power Sources 260 (2014) 276 – 291.

[12] C. Fleischer, W. Waag, H.-M. Heyn, D. U. Sauer, On-line adaptive battery impedance parameter and state estimation considering physical principles in reduced order equivalent circuit battery models: Part 2. Parameter and state estimation, J. Power Sources 262 (2014) 457 – 482.

[13] Application note #49. EIS measurements: Potentio (PEIS) or Galvano (GEIS) mode, that is the question.

[14] Application note #23. EIS measurements on Li-ion batteries EC-Lab® software parameters adjustment.

[15] Application note #42. ZFit: The modified inductance element La.

[16] Application note #43. How to fit transmission lines with ZFit.

[17] Technical note #16. Influence of the temperature for impedance measurements.

[18] S.S. Zhang, K. Xu, T.R. Jow, Electrochemical impedance study on the low temperature of Li-ion batteries, Electrochim. Acta 49 (7) (2004) 1057 – 1061.

[19] H. C. Shin, W. I. Cho, H. Jang, Electrochemical properties of the carbon-coated LiFePO4 as a cathode material for lithium-ion secondary batteries, J. Power Sources 159 (2) (2006) 1383 – 1388.

[20] J. Li, E. Murphy, J. Winnick, P. Kohl, Studies on the cycle life of commercial lithium ion batteries during rapid charge-discharge cycling, J. Power Sources 102 (12) (2001) 294 – 301.

[21] M. Umeda, K. Dokko, Y. Fujita, M. Mohamedi, I. Uchida, J. Selman, Electrochemical impedance study of Li-ion insertion into mesocarbon microbead single particle electrode: Part I. Graphitized carbon, Electrochim. Acta 47 (6) (2001) 885 – 890.

[22] Etude de reactions electrochimiques par SIE. Reactions d'insertion

[23] C. Delacourt, M. Ati, J. M. Tarascon, Measurement of lithium diffusion coefficient in $LiFeSO_4F$, J. Electrochem. Soc. 158 (2011) A741–A749.

[24] A. Martinent, B. Le Gorrec, C. Montella, R. Yazami, Three-electrode button cell for {EIS} investigation of graphite electrode, J. Power Sources 97 - 98 (2001) 83 – 86, proceedings of the 10th International Meeting on Lithium Batteries.

[25] M. Dollé, F. Orsini, G.A.S., J.-M. Tarascon, Development of reliable three-electrode impedance measurements in plastic Li-ion batteries, J. Electrochem. Soc. 148 (2001) A851–A857.

[26] M. Klett, J. A. Gilbert, S. E. Trask, B. J. Polzin, A. N. Jansen, D. W. Dees, D. P. Abraham, Electrode behavior re-visited: Monitoring potential windows, capacity loss, and impedance changes in Li1.03(Ni0.5Co0.2Mn0.3)0.97O2/silicon-graphite full cells, J. Electrochem. Soc. 163 (6) (2016) A875–A887.

[27] Application Note #61. How to interpret lower frequencies impedance in batteries ?

[28] Application Note #62. How to measure the internal resistance of a battery using EIS ?

[29] Application Note #58. Cycling battery with reference electrode by using the PAT-cell test cell.

[30] J.-P. Diard, C. Montella, Non-intuitive features of equivalent circuits for analysis of EIS data. The example of EE reaction, J. Electroanal. Chem. 735 (2014) 99 – 110.